RNA binding is more critical to the suppression of silencing function of *Cucumber mosaic virus* 2b protein than nuclear localization

INMACULADA GONZÁLEZ,[1,7] DARIA RAKITINA,[2,7] MARIA SEMASHKO,[2] MICHAEL TALIANSKY,[3] SHELLY PRAVEEN,[4] PETER PALUKAITIS,[5] JOHN P. CARR,[6] NATALIA KALININA,[2] and TOMÁS CANTO[1,8]

[1]Centro de Investigaciones Biológicas, CIB, CSIC, Madrid 28040, Spain
[2]A. N. Belozersky Institute of Physico-Chemical Biology, Biological Faculty, Moscow State University, Leninskye Gory 119991, Russia
[3]The James Hutton Institute, Invergowrie, Dundee DD2 5DA, Scotland, United Kingdom
[4]Indian Agricultural Research institute, New Delhi 110-012, India
[5]Seoul Women's University, Seoul 139-774, South Korea
[6]Department of Plant Sciences, University of Cambridge, Cambridge CB2 3EA, United Kingdom

ABSTRACT

Previously, we found that silencing suppression by the 2b protein and six mutants correlated both with their ability to bind to double-stranded (ds) small RNAs (sRNAs) in vitro and with their nuclear/nucleolar localization. To further discern the contribution to suppression activity of sRNA binding and of nuclear localization, we have characterized the kinetics of in vitro binding to a ds sRNA, a single-stranded (ss) sRNA, and a micro RNA (miRNA) of the native 2b protein and eight mutant variants. We have also added a nuclear export signal (NES) to the 2b protein and assessed how it affected subcellular distribution and suppressor activity. We found that in solution native protein bound ds siRNA, miRNA, and ss sRNA with high affinity, at protein:RNA molar ratios ~2:1. Of the four mutants that retained suppressor activity, three showed sRNA binding profiles similar to those of the native protein, whereas the remaining one bound ss sRNA at a 2:1 molar ratio, but both ds sRNAs with 1.5–2 times slightly lower affinity. Three of the four mutants lacking suppressor activity failed to bind to any sRNA, whereas the remaining one bound them at far higher ratios. NES-tagged 2b protein became cytoplasmic, but suppression activity in patch assays remained unaffected. These results support binding to sRNAs at molar ratios at or near 2:1 as critical to the suppressor activity of the 2b protein. They also show that cytoplasmically localized 2b protein retained suppressor activity, and that a sustained nuclear localization was not required for this function.

Keywords: CMV 2b protein; RNA silencing suppression; small RNA binding; subcellular localization of viral proteins

INTRODUCTION

The 2b protein of *Cucumber mosaic virus* (CMV) is the smallest of the five gene products encoded by this tripartite, positive stranded RNA virus. This protein was among the first viral proteins identified as a suppressor of RNA silencing (Brigneti et al. 1998). Cell fractionation studies of infected plant tissues showed that, during the course of viral infection, CMV 2b protein accumulated mainly within the cell nucleus, apparently in insoluble inclusions (Mayers et al. 2000). Cell biology studies using CMV 2b protein tagged with reporter markers confirmed its predominantly nuclear nature in a CMV-free environment (Lucy et al. 2000; Wang et al. 2004), and more recently it was found that, within the nucleus, fluorescently tagged protein that retained silencing suppressor activity accumulated in the nucleolus (González et al. 2010).

CMV 2b protein was shown to bind to small RNAs (sRNAs), such as double-stranded (ds) short-interfering RNAs (siRNAs) or micro RNAs (miRNAs) in vitro (Goto et al. 2007; Rashid et al. 2008; González et al. 2010), to siRNAs in vivo (Kanazawa et al. 2011), and recently to miRNAs, also in vivo (Hamera et al. 2012). The kinetics of binding of the protein to each of these types of RNAs in vitro have not been determined, but binding to siRNAs has been proposed to be the means by which the protein interferes with antiviral RNA silencing (Goto et al. 2007;

[7]These authors contributed equally to this work.
[8]**Corresponding author.**
E-mail tomas.canto@cib.csic.es.
Article published online ahead of print. Article and publication date are at http://www.rnajournal.org/cgi/doi/10.1261/rna.031260.111.

González et al. 2010). In addition, the 2b protein homolog from the cucumovirus *Tomato aspermy virus* (TAV) has been shown to bind to siRNAs, miRNAs, and longer single-stranded (ss) RNAs in vitro (Rashid et al. 2008) and also to viral RNAs in vivo (Shi et al. 2008). Besides binding to sRNAs, CMV 2b protein could interact with protein components of the RNA silencing machinery: It could bind to Argonaute (AGO) proteins 1 and 4 in planta (Zhang et al. 2006; González et al. 2010; Hamera et al. 2012). AGO proteins are components of the specific RNA-induced silencing complexes (RISC), some of which take part in antiviral defense. It has been proposed that interaction of 2b with AGO1 could inhibit RISCs involved in antiviral RNA silencing (Zhang et al. 2006) and that AGO4 activity is negatively affected by its interaction with 2b protein (Hamera et al. 2012). Besides these direct interactions with AGO proteins, transcription of AGO4 mRNA has been shown to be negatively affected by the 2b protein (Cillo et al. 2009; Ye et al. 2009). It is therefore probable that the 2b protein neutralizes at least two different levels of antiviral RNA silencing by binding to siRNAs and host proteins.

Despite its small size, of just 110 amino acids in the case of strain Fny CMV, the interactome of the 2b protein established so far also includes factors that are not components of the silencing machinery. Fny CMV 2b interacts in the yeast-two-hybrid system with the importin-like nuclear transport factor karyopherin α (Wang et al. 2004), which could be involved in the transport of 2b protein into the nucleus. Recently, it was shown that the 2b protein from CMV strain HL can interact both in the yeast-two-hybrid system and in planta with a cytoplasmic host catalase (CAT3), inhibiting its H_2O_2 scavenging activity and thus allowing the appearance of systemic necrosis in infected *Arabidopsis thaliana* Col 0 plants. The HL-CMV 2b protein also relocates CAT3 to the nucleus, although this seems not to be required for the onset of necrosis (Inaba et al. 2011).

In addition to these interactions of the 2b protein with host proteins and nucleic acids, it is also known that the 2b protein stimulates salicylic acid accumulation but interferes with the host's salicylic acid- and jasmonic acid-mediated resistance responses (Ji and Ding 2001; Lewsey et al. 2010). The protein also interferes with the long-range signaling of silencing in the plant (Guo and Ding 2002), with the accumulation of siRNAs generated by the plant DICER-like proteins 2, 3, and 4 (Díaz-Pendón et al. 2007), with the metabolism of some miRNAs involved in development (Lewsey et al. 2007; Cillo et al. 2009), and also with transgene DNA methylation (Guo and Ding 2002). The ability of the 2b protein to facilitate the transit of sRNAs into the nucleus has also been demonstrated recently and used to facilitate inheritable epigenetic modifications of endogenous plant gene promoters, using dsRNAs originating from a CMV-derived vector (Kanazawa et al. 2011).

Studies using the TAV 2b protein homolog showed that in aqueous solution it spontaneously formed homodimers, even in the absence of sRNAs. In the presence of ds sRNAs, a TAV 2b homodimer interacted in vitro in a length-specific, non-sequence-specific manner with a single RNA molecule (Chen et al. 2008; Rashid et al. 2008). These sRNA-bound homodimers spontaneously adopted a tetrameric form through the leucine zipper-like motifs present at the protein N terminus. Crystallographic analysis showed that in this conformation the 2b sequence contains two main α-helix structures separated by a short linking region. These two α-helices formed hook-like structures that interacted with the sRNA (Chen et al. 2008). In the case of CMV, 2b proteins with reporter sequences fused to the N termini, which would likely prevent tetramerization, remained fully functional as suppressors of silencing in patch assays, suggesting that tetramerization is not needed for suppression of local silencing (González et al. 2010).

In the Fny CMV 2b protein sequence there are two putative nuclear localization signals (NLS) (amino acids 22–27 and 33–36, both present in the first α-helix) and a putative phosphorylation site (amino acids 39–43) located at the end of the linking region and the beginning of the second α-helix (Wang et al. 2004). These two NLS regions are responsible for the predominantly nuclear localization of the protein. The effect of a battery of mutations affecting these motifs and also other regions of the 2b protein on virus infectivity was determined by Lewsey et al. (2009). The effect of these mutations on the 2b protein subcellular localization pattern, on its ability to interact with proteins in vivo or with synthetic siRNAs in vitro, and on suppression of silencing activity in patch assays was determined by González et al. (2010). The latter found that lack of suppression of silencing correlated strongly with inability to bind to synthetic siRNAs in vitro and with altered subcellular targeting. However, since the NLS and phosphorylation domains overlap with α-helix regions involved in the binding to sRNAs, it was not possible to discern the relative importance of these subcellular targeting of nuclei/nucleoli vs. siRNA binding properties in the protein suppressor function. Here, we have examined the relative importance to the RNA silencing suppressor activity of the 2b protein of sRNA binding vs. nuclear targeting.

RESULTS

In vivo characterization of 2b protein mutants

To ascertain the relative contribution to silencing suppression by the 2b protein of sRNA binding vs. nuclear localization, we designed two new mutant proteins with changes to the protein sequences lying outside the region of the protein directly involved in binding to sRNAs (González et al. 2010). The first mutant had a deletion of four amino acids Gly–Ser–Glu–Leu (2bΔGSEL) at positions 62–65 of the 2b protein. This conserved region belongs to a small α-helical domain (Domain 3) in the 2b protein homolog

encoded by the SD strain of CMV that has been shown to be important for the strength of its silencing suppressor activity and for the down-regulation of the levels of *AGO4* mRNA during viral infection (Ye et al. 2009). The second deletion mutant lacked the C-terminal 16 amino acids of the 2b protein (2bΔ3T) (Lewsey et al. 2009).

In patch assays, both mutants were able to suppress the partial silencing of a *green fluorescent protein* (*GFP*) reporter gene when co-expressed transiently in *Nicotiana benthamiana* leaf tissue from agroinfiltrated binary vectors (Fig. 1A). The two mutants also were tagged with GFP at their N termini to study their subcellular distribution by confocal laser scanning microscopy (constructs GFP–2bΔGSEL and GFP–2bΔ3T). The GFP sequence fused to the 2b protein did not affect the suppressor activity of either the native protein (González et al. 2010) or these two mutants (data not shown). The subcellular distributions of GFP–2bΔGSEL and of GFP–2bΔ3T were similar to that of the native 2b protein: Both mutants were present throughout the cytoplasm and inside the nucleus, retaining the ability to target the nucleolus (Fig. 1B. Nu, arrows). Nucleoli were identified by co-expression with fibrillarin tagged with monomeric red fluorescent protein (data not shown; see González et al. 2010). In *N. benthamiana* plants, infection with mutant CMV expressing 2bΔ3T causes slightly altered symptoms with increased severity (Lewsey et al. 2009). In the same host, CMV carrying the 2b protein mutant ΔGSEL caused attenuated virus infection symptoms relative to the wild-type (wt) virus, but virus titers were only marginally lower than wt virus (Fig. 1C). A summary of the properties of the native 2b protein plus the eight mutants described in previous works (Lewsey et al. 2009; González et al. 2010) and in this work is shown in Table 1. A schematic representation of the different mutants is shown in Figure 2A.

Kinetic parameters of the binding in vitro of the 2b protein and eight mutant variants to three types of sRNAs and a viral RNA

The ability of the CMV 2b protein to bind to sRNAs in vitro had been demonstrated previously (Goto et al. 2007; Rashid et al. 2008; Shimura et al. 2008), and the affinity of an *Escherichia coli*–expressed 2b protein tagged with maltose-binding protein (MBP-2b) for a 3′ biotinylated siRNA in vitro was also determined (Shimura et al. 2008). Furthermore, using a battery of six 2b protein mutants a correlation between ability to bind to siRNAs in vitro and suppressor activity had been found (González et al. 2010). However, no detailed characterization of the kinetics of binding of native and mutant CMV 2b proteins that had been biologically characterized to different kinds of sRNAs in vitro had yet been made. We determined the kinetics of binding of the native 2b protein and of eight mutant variants (2bΔNLS1; 2bΔNLS2; 2bΔNLS1 + 2; 2bΔKSPSE; 2bS40A; 2bS42A; 2bΔGSEL, and 2bΔ3T) (Fig. 2A,B) to three different types of synthetic sRNAs (a ds siRNA; an ss sRNA, and an miRNA), all sharing the sequence of miRNA 171 (Fig. 2C), as well as to the genomic ss RNA of *Tobacco mosaic virus* (TMV).

Histidine-tagged versions of the native and eight mutant 2b proteins were expressed in *E. coli*, and the purified renatured soluble proteins were used in electrophoretic mobility shift assays (EMSA) in vitro. RNA-binding data are given as binding curves obtained from the EMSA results. The percentage of RNA retained after interaction with increasing amounts of protein is plotted against the protein:RNA molar ratio for each of the four RNA substrates (Figs. 3, 4). EMSA gels in the case of the interaction of the 2b protein and eight mutants with the ds siRNA are also shown (Fig. 3).

Our results demonstrate that native 2b protein interacted with ds siRNA with an apparent dissociation constant (K_d) value of 0.92 μM in a cooperative manner (Hill coefficient of 3.65). Nearly 60% of the ds siRNA molecules were com-

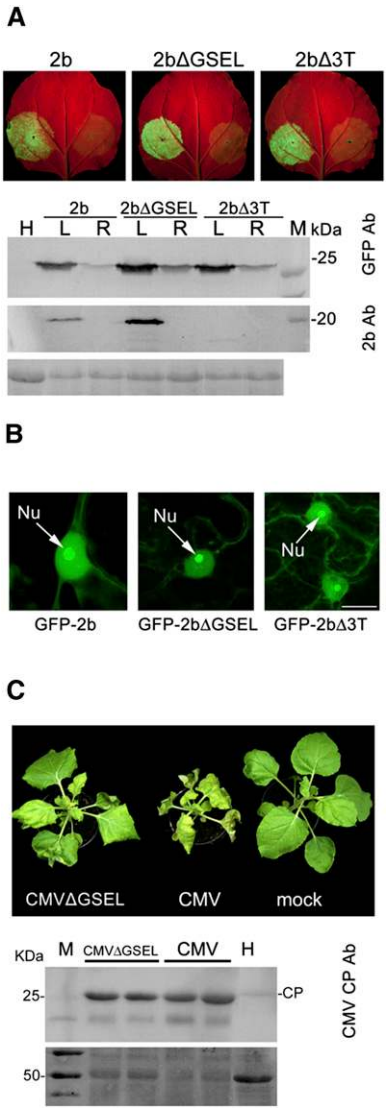

FIGURE 1. (Legend on next page)

plexed with 2b protein at a protein:RNA molar ratio of 2:1 (Fig. 3; Table 2). This molar ratio agrees with the structural data from the related TAV 2b protein complex, where the 2b protein bound sRNAs as a dimer (Chen et al. 2008). The native protein also bound effectively to the ss sRNA and to the miRNA (apparent K_d values of 1.61 μM and 1.23 μM; Hill coefficients ~2.03 and 2.11, respectively) (Fig. 4; Table 2). It is interesting to note that >80% of ss sRNA was retained at a protein:RNA molar ratio of 2:1, whereas only 40% of the miRNA was bound by the 2b protein at the same molar ratio.

Four of the eight mutant proteins tested (2bS40A, 2bS42A, 2bΔGSEL, and 2bΔ3T) retained silencing suppressor activity (Table 1). Interestingly, three of them (2bS40A, 2bΔGSEL, and 2bΔ3T) showed higher affinities for the synthetic sRNAs than the native 2b protein (Figs. 3, 4). The apparent K_d values for these three mutants were twofold higher: 80%–100% of ds siRNA or ss sRNA and 70%–90% of miRNA were involved in complexes with the mutant proteins at a protein:RNA molar ratio of 2:1 (Figs. 3, 4; Table 2). Interestingly, deletions in the C-terminal half of the protein (constructs 2bΔGSEL and 2bΔ3T) seem to have made RNA-binding more efficient. In contrast, the RNA binding characteristics of the remaining mutant, 2bS42A, were weaker than those of the native protein or of the other three mutants that retained suppressor activity: At a molar ratio of 2:1 it retarded only 25% of ds siRNA and <5% of miRNA, although it was as efficient as the native 2b protein in its interaction with the ss sRNA (Figs. 3, 4; Table 2). In the case of the four mutants without suppressor activity (2bΔNLS1, 2bΔNLS2, 2bΔNLS1 + 2, and 2bΔKSPSE), the first three showed no binding to any of the sRNAs (Figs. 3, 4; Table 2), whereas the 2bΔKSPSE mutant still retained some RNA-binding activity. However, the affinity of this mutant to any of the sRNAs was low compared with the native 2b protein. For example, the apparent K_d of the 2bΔKSPSE mutant to ds siRNA was 4.63 μM, vs. 0.92 μM for the native 2b protein. This mutant showed no retardation of ds siRNA and miRNA at a molar ratio of 2:1 (50% binding of these RNA was achieved at molar ratios of 8–10:1) and also had low affinity to the ss sRNA (Figs. 3, 4; Table 2).

Our results therefore show that the binding of native 2b and of the eight mutant variants to the three types of synthetic sRNAs could be broadly grouped into four main patterns. Pattern 1 was observed for the native protein and three of the four proteins that retained suppression of silencing activity (2b, 2bS40A, 2bΔGSEL, 2bΔ3T). Pattern 2 was observed for the remaining mutant 2bS42A with silencing suppression activity. In the case of the four constructs without suppressor activity (2bΔNLS1, 2bΔNLS2, 2bΔNLS1 + 2, and 2bΔKSPSE) the first three showed no binding to any of the three sRNAs at any molar ratio (pattern 3), whereas noneffective but cooperative binding was observed for 2bΔKSPSE (pattern 4). Therefore, analysis of the eight 2b mutants points to a correlation between suppressor activity and the ability to bind sRNAs effectively (patterns 1 and 2).

The 2b protein also was able to interact cooperatively with TMV genomic RNA (~6.4 kilobases [kb]). The apparent K_d for TMV RNA binding was 1.78 μM. Full retardation occurred at a protein:RNA molar ratio of 500:1 and the Hill coefficient was 1.72 (Table 2). Binding of the eight 2b protein mutant variants to TMV RNA followed only two patterns: All constructs with biological activity as suppressors in patch assays (constructs 2bS40A, 2bS42A, 2bΔGSEL, 2bΔ3T) interacted with TMV RNA similarly to the native 2b protein. The four constructs that had no suppressor activity (constructs 2bΔNLS1, 2bΔNLS2, 2bΔNLS1 + 2, and 2bΔKSPSE) showed very weak ability to bind TMV RNA, achieving <30% retention at a molar ratio of 1000:1 (Fig. 4, bottom chart).

The effect of the attachment of a nuclear export signal to the 2b protein on its subcellular localization and suppression of silencing activity in patch assays

Deletion of either or both of the NLSs of the 2b protein of Fny CMV reduced or prevented the accumulation of the protein in the nucleus (Lucy et al. 2000; Wang et al. 2004; González et al. 2010). It also abolished its suppression of

FIGURE 1. In vivo characterization of 2b protein deletion mutants 2bΔGSEL and 2bΔ3T and of their biological activities. (*A*) Suppression of RNA silencing in patch assays. A binary vector expressing the *Aquorea victoria green fluorescent protein* (*GFP*) reporter gene was agroinfiltrated into *N. benthamiana* leaves, together with an empty binary vector (infiltrated patch on *right* side of leaves) or together with binary vectors expressing 2b protein (infiltrated patch on *left* side of the *left* leaf), 2bΔGSEL (infiltrated patch on *left* side of the *middle* leaf) or 2bΔ3T (infiltrated patch on *left* side of *right* leaf). All three 2b constructs suppressed the partial silencing of the *GFP* reporter gene, increasing the levels of GFP-derived green fluorescence when leaves were illuminated with UV light, 3 d after infiltration (infiltrated patches in *left* vs. *right* side of leaves). Increased GFP levels in the presence of the suppressors were confirmed by Western blot analysis using a GFP antibody (*upper* gray panel). The presence of the 2b suppressors also was confirmed by Western blot analysis using a 2b antibody (*middle* gray panel). Note that, because the 2b mouse antibody was raised against two synthetic peptides at the N and C terminus of the 2b protein (González et al. 2010) and 2bΔ3T has the last 16 amino acids deleted, its accumulation could be underestimated with this antibody. Lanes labeled *L* and *R* correspond to the infiltrated patches on *left* and *right* side of leaves, respectively. The *lower* gray panel is a control of loading. (*B*) Subcellular distribution of GFP–2b, GFP–2bΔGSEL, and of GFP–2bΔ3T. In epidermal cells of agroinfiltrated *N. benthamiana* leaves, all three constructs targeted the nucleus and, inside it, the nucleolus (Nu, arrows). Bar in the *lower right* corner represents 10 μm. (*C*) Symptoms induced by CMV expressing 2bΔGSEL vs. those induced by wt Fny CMV. Symptoms were less severe than those induced by the wt virus (*upper* panel, *left* vs. *central* plant). Western blot analysis of viral CP amounts in infected tissue showed that virus expressing 2b ΔGSEL accumulated only slightly less CP than wt virus (*middle* panel) in those plants. Each lane represents one independent leaf sample. (Lane *H*) Extract from healthy plant tissue; (lane *M*) molecular weight markers. The *lower* panel shows the Ponceau S-stained membrane used in the inmunoblot as control of loading.

TABLE 1. Summary of the properties of Fny CMV 2b protein, and of the eight mutant variants described in previous work and in this paper

	Nucleolar presence[a]	In vitro binding to sRNAs[a]	Silencing suppressor activity[a]	Viral infection symptoms in *N. benthamiana*
2b	+	+	+	Stunting, leaf distortion, necrosis[b]
2bΔNLS1 (22–27)	–	–	–	Asymptomatic[b]
2bΔNLS2 (33–36)	+/– [c]	–	–	Asymptomatic[b]
2bΔNLS1 + 2	–	–	–	Asymptomatic[b]
2bΔKSPSE (39–43)	+++ [d]	+/– [e]	–	Asymptomatic[b]
2bΔS40A	+	+	+	Mild stunting, mild leaf distortion[b]
2bΔS42A	+	+	+	Intermediate stunting, intermediate leaf distortion[b]
2bΔGSEL (62–65)	+	+	+	Intermediate leaf distortion[a]
2bΔ3T (95–110)	+	+	+	Stunting, leaf distortion, necrosis[b]

[a]From González et al. 2010 and this work.
[b]From Lewsey et al. 2009.
[c]Very limited nucleolar presence.
[d]Mainly nucleolar.
[e]Only at protein:RNA molar ratios above 14:1.

silencing activity and for this reason nuclear localization of the 2b protein has been linked to its suppression of silencing function (Lucy et al. 2000; González et al. 2010). However, this could also be caused by the fact that both NLSs are located in the two regions in the homodimer that are known to interact with siRNAs. To discriminate between the contribution of the nuclear localization and siRNA binding activity to the suppressor function, we took advantage of the fact that the 2b protein is amenable to accepting diverse tags at either its N or C termini, without having its suppressor activity compromised in patch assays (González et al. 2010). We thus fused a nuclear export signal (NES) from a protein kinase inhibitor (PKI: Wen et al. 1995; García et al. 2009) to the N terminus of a biologically active GFP–2b fusion protein (González et al. 2010), generating a NES–GFP–2b fusion protein. This NES motif has been shown to work efficiently in plants. Both GFP–2b and NES–GFP–2b were expressed transiently in *N. benthamiana* epidermal cells by agroinfiltration, and their corresponding subcellular distribution patterns, as well as their ability to suppress the silencing of a reporter *GFP* gene, were monitored in time course experiments from 3 to 6 d post-infiltration (dpi). From the start of the observations, both proteins showed differences in their subcellular distribution, with fluorescence derived from NES–GFP–2b absent from most nuclei (Fig. 5A). A comparative quantitative study using fields of cells in infiltrated patches for each construct and at each of the four times post-infiltration studied showed that, in contrast to what was observed for GFP–2b, >90% of nuclei were devoid of NES–GFP–2b as early as 3 dpi, a percentage that increased further at 4, 5, and 6 dpi (Fig. 5B). The ability of the two constructs to suppress the silencing of a free *GFP* reporter gene was followed at 3, 4, 5, and 6 dpi, and it was found that suppressor activity was not affected by the cytoplasmic localization of NES–GFP–2b (Fig. 6A,B). A quantitative analysis of the increase in the amount of free GFP in infiltrated patches relative to the amount of suppressor in the tissue confirmed that suppressor activities of both NES–GFP–2b and GFP–2b were comparable (Fig. 6B,C). This also was the case in a sequential infiltration patch assay in which the suppressors were infiltrated three days before the *GFP* reporter (Fig. 7).

DISCUSSION

Initial cell biology studies had linked nuclear targeting of the 2b protein to its pathogenicity determinant nature (Lucy et al. 2000). Those initial reports on the requirement for nuclear localization for the 2b protein suppressor function had suggested a role of the protein as a competitor in nuclear transport or in transcriptional regulation (Lucy et al. 2000), or in interference with nuclear DNA methylation (Guo and Ding 2002). However, nuclear accumulation alone was not sufficient to confer 2b-mediated silencing suppression, and it was proposed that the NLS motifs could have a role leading to pathogenicity enhancement different to that of transporting the protein into the nucleus (Wang et al. 2004).

Recent structural studies on the TAV homolog of CMV 2b confirmed that the NLS domains were indeed involved in a role other than nuclear translocation: Upon binding to siRNAs, the 2b protein of TAV adopted a structure in which both NLSs were immersed in the first of two α-helices directly involved in binding to siRNAs, whereas the phosphorylation motif was immersed in the second α-helix (Chen et al. 2008; Rashid et al. 2008). Therefore, it could be expected that alterations in amino acids within these structures could prevent siRNA binding, and this turned out to be the case. Thus, deletions of either or in both of the NLS motifs not only prevented or abolished nuclear accumulation of the 2b protein, but at the same time prevented binding to siRNAs and the suppression of silencing by the 2b protein (Goto et al. 2007; Rashid et al. 2008; González et al. 2010). Likewise, deletion of the phosphorylation motif in the second α-helix altered the protein's subcellular localization, confining it largely to the nucleolus, while at the same time this mutation abolished siRNA binding in vitro, and with it silencing suppression

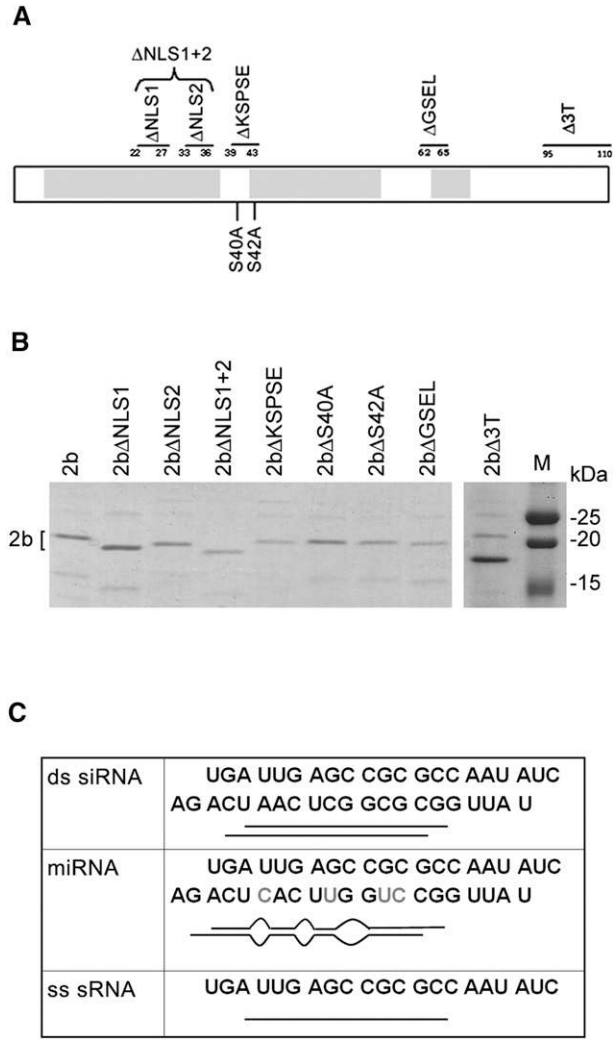

FIGURE 2. (*A*) Schematic representation of the 110-amino acid 2b protein of Fny CMV, with the amino acid positions of the eight mutants used in this work (six deletion mutants and two alanine substitution mutants) and their names indicated. The gray boxes indicate the main regions of the 2b protein expected to adopt α-helical conformation in the homodimer (following Chen et al. 2008 and Ye et al. 2009). (*B*) Expression and isolation of 2b protein and eight mutant variants in bacteria. N-terminal 6×Histidine-tagged and C-terminal HA-tagged native 2b protein and eight 2b protein mutant variants were expressed in *E. coli*, renatured and purified using Ni-NTA resin. Protein amounts were then quantified using SDS-PAGE gels against known protein standards. (*C*) To perform a comparative study on the kinetics of binding of the 2b protein and its variants to different types of synthetic sRNAs, a ds siRNA, a ss sRNA, and a miRNA were used, all sharing the sequence of miRNA 171.

(González et al. 2010). Therefore, data on the TAV 2b structure as well as on the siRNA binding properties of the 2b protein of both TAV and CMV suggested that siRNA binding was involved in the suppression function and that the alteration in the nuclear targeting in 2b deletion mutants was a side effect and not the cause of their lack of suppressor activity (Goto et al. 2007; Chen et al. 2008; Rashid et al. 2008; González et al. 2010). This issue had not been elucidated to date, and in this work we have addressed the relative contributions to the 2b protein-mediated silencing suppression function of its subcellular targeting to nuclei and nucleoli vs. its sRNA binding properties. To do this, we compared the abilities of the wt 2b protein and of eight mutant variants to bind in vitro to three types of sRNAs that share the sequence of miRNA 171, and also to the 6.4-kb TMV ss RNA, and determined the kinetic parameters of their RNA binding. These mutations were distributed throughout the whole of the protein and targeted areas that have been linked to various 2b protein functions: the suppression of silencing, such as those affecting the NLS 1 and NLS 2 domains, 2bΔNLS1, 2bΔNLS2, 2bΔNLS1 + 2 (Lucy et al. 2000; Wang et al. 2004;

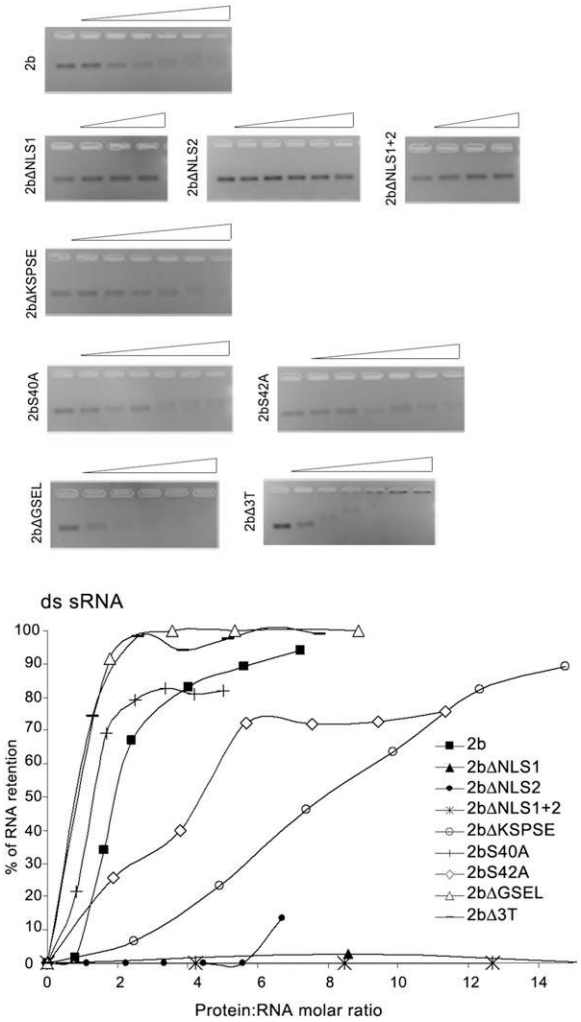

FIGURE 3. EMSA for the binding of 2b protein and eight mutant variants to a miRNA 171 sequence-based synthetic ds siRNA using nondenaturing 2% agarose gels. Agarose gels from which data were obtained are shown as an example. In each gel lane RNAs were incubated with either no protein (as control, first lane from the *left* of each gel) or with increasing volumes of 2b protein (second lane from the *left* onward). The chart shows the percentage of retarded siRNA plotted against the protein:RNA molar ratio in the samples.

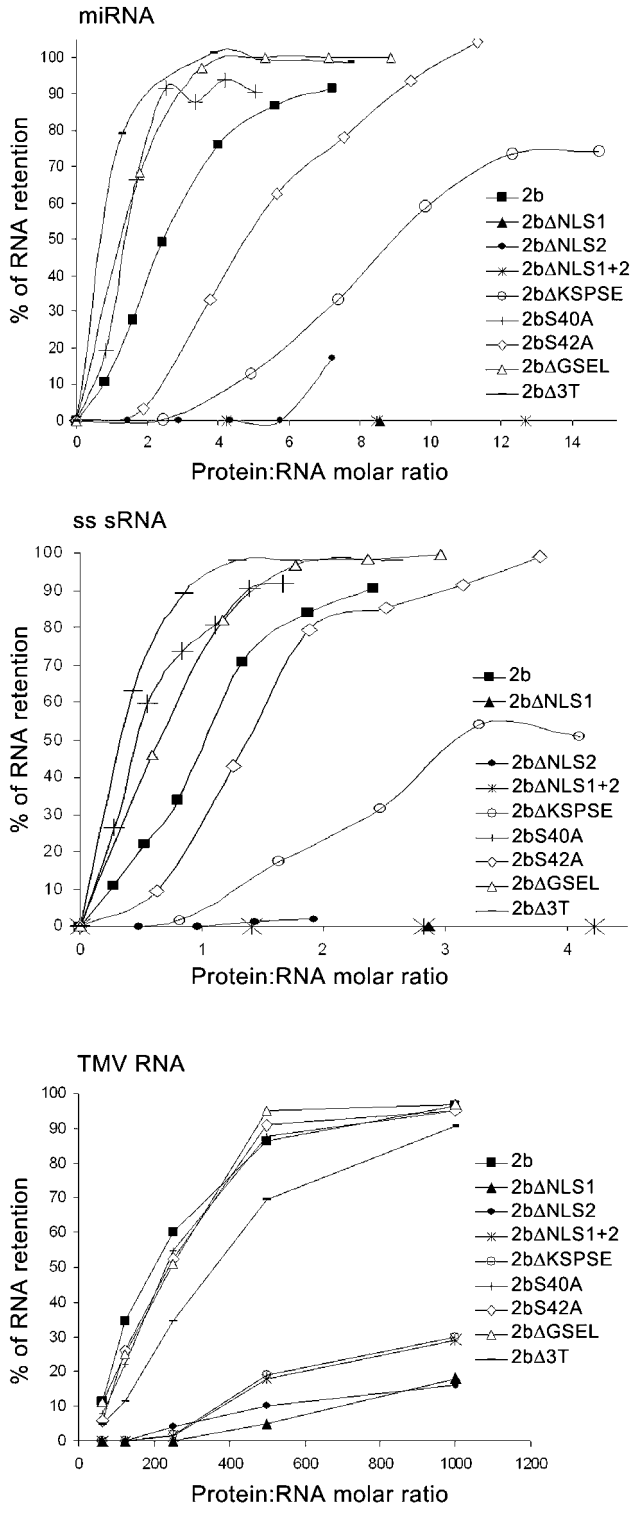

FIGURE 4. EMSA for the binding of 2b protein and eight mutant variants to a synthetic miRNA 171, to a miRNA 171 sequence-based synthetic ss sRNA using nondenaturing 2% agarose gels (*upper* and *middle* charts, respectively), and of 2b protein and eight mutant variants to a TMV viral RNA using a 0.8% nondenaturing agarose gel (*lower* chart). RNAs were incubated with either no protein as control or with increasing volumes of 2b protein. The percentage of retarded RNA is plotted against the protein:RNA molar ratio in the sample.

Goto et al. 2007; Rashid et al. 2008; Lewsey et al. 2009; González et al. 2010); the putative protein phosphorylation site, 2bΔKSPSE, 2bS40A, 2bS42A (Lewsey et al. 2009; González et al. 2010); the domain involved in the down-regulation of *AGO4* mRNA, 2bΔGSEL (Ye et al. 2009), and the C-terminal region, 2bΔ3T (Lewsey et al. 2009).

Our results showed that up to 60% of ds siRNA could be bound to the recombinant native 2b protein in solution at a protein:RNA molar ratio ~2:1 (Fig. 3). These results are in agreement with the structural model of the TAV2b–sRNA complex (Chen et al. 2008) and the binding data of labeled RNAs to Chip-immobilized TAV 2b protein (Rashid et al. 2008). We have also shown that the 2b protein can interact in vitro with miRNA and ss sRNA with similar affinity and molar ratios. Our results are in agreement with recent data from Hamera et al. (2012). A weaker 2b protein binding affinity for miRNA reported previously (Goto et al. 2007) could be connected to either properties of the 2b protein belonging to another CMV strain (CMV 95R) or differences in experimental conditions.

Analysis of the eight 2b mutants points to a correlation between suppressor activity and the ability to bind sRNAs effectively. The four mutants that retained suppressor activity (2bS40A, 2bS42A, 2bΔGSEL, and 2bΔ3T) showed sRNA binding similar to or stronger than that of the native 2b protein. Two of the mutants that showed stronger binding affinities to sRNAs than the native 2b protein (2bΔGSEL and 2bΔ3T) contained a deletion of either the C-terminal 16 amino acids (2bΔ3T) or the first four amino acids (2bΔGSEL) of the third, smaller, nine-amino acid α-helix (Domain 3 of Ye et al. 2009). The C-terminal 16 amino acids of the 2b protein were shown to have transcription activation activity in yeast (Ham et al. 1999), and elimination of the C terminus from the 2b protein (or alteration of amino acid 104) attenuated the toxicity associated with overexpression of the 2b protein in *E. coli*, as well as reduced the ability of the 2b protein to bind DNA in vitro (Sueda et al. 2010). Deletion of these sequences also led to enhanced pathogenicity in some infected host plants (Lewsey et al. 2009), which may be due to the increased affinity for sRNAs. The 2bΔGSEL mutant may have affected the stability of the third α-helix, the role of which is unknown, although deletion of the third α-helix (amino acids 64–71) led to a 19-fold reduction is silencing suppression of GFP in SD CMV 2b protein (Ye et al. 2009), whereas deletion of amino acids 62–65 (2bΔGSEL) in Fny CMV 2b protein did not affect RNA silencing (Fig. 1). Why deletion of the amino acids 62–65 increased RNA binding is also unknown.

Three of the four mutants lacking suppressor activity failed to bind in vitro to sRNAs (mutants 2bΔNLS1, 2bΔNLS2, 2bΔNLS1 + 2), whereas the remaining one (mutant 2bΔKSPSE), with a deletion in a putative phosphorylation site and a strong nucleolar localization, still binds to sRNAs, albeit with low affinity and at much higher molar ratios (Figs. 3, 4; Table 2). It is interesting to compare the three

TABLE 2. Kinetic parameters observed in the binding of 2b protein to various RNAs

	ds siRNA		miRNA		ss sRNA		TMV RNA	
	Apparent K_d (μM)	Hill coeff.	Apparent K_d (μM)	Hill coeff.	Apparent K_d (μM)	Hill coeff.	Apparent K_d (μM)	Hill coeff.
2b	0.92 ± 0.03	3.65 ± 0.41	1.23 ± 0.05	2.11 ± 0.13	1.61 ± 0.28	2.03 ± 0.40	1.78 ± 0.17	1.72 ± 0.13
2bΔNLS1	NO	NO	NO	NO	NO	NO	NO	NO
2b ΔNLS2	NO	NO	NO	NO	NO	NO	NO	NO
2bΔNLS1 + 2	NO	NO	NO	NO	NO	NO	NO	NO
2bΔKSPSE	4.63 ± 0.39	2.26 ± 0.19	3.96 ± 0.17	4.03 ± 0.56	5.61 ± 1.17	2.7 ± 0.74	NO	NO
2bS40A	0.55 ± 0.07	3.88 ± 0.15	0.62 ± 0.03	3.48 ± 0.47	0.71 ± 0.04	1.85 ± 0.18	2.00 ± 0.11	2.20 ± 0.21
2bS42A	1.59 ± 0.36	1.9 ± 0.77	2.80 ± 0.01	2.55 ± 0.33	2.00 ± 0.09	3.23 ± 0.46	2.01 ± 0.26	2.12 ± 0.43
2bΔGSEL	0.58 ± 0.09	5.66 ± 2.11	0.73 ± 0.01	3.91 ± 0.15	0.98 ± 0.03	2.38 ± 0.21	2.11 ± 0.40	2.02 ± 0.57
2bΔ3T	0.47 ± 0.01	2.9 ± 0.01	0.39 ± 0.06	2.69 ± 0.83	0.52 ± 0.02	2.51 ± 0.29	3.10 ± 0.14	2.01 ± 0.11

Apparent dissociation constants K_d and Hill coefficients (>1, cooperative binding) were obtained for the binding in vitro of 2b protein and eight 2b mutant variants to three types of small RNAs (sRNAs: a double-stranded sRNA, a single-stranded sRNA, and a micro [mi] RNA, all sharing the miRNA 171 sequence), as well as to a 6.4-kb full-length viral RNA from *Tobacco mosaic virus* (TMV). (NO) Not obtained, i.e., the protein showed no (or marginal) RNA-binding, and, therefore, no kinetic parameters were calculated. Values are averages for three individual experiments. Standard deviations are given for apparent K_d and Hill coefficients.

mutants with the putative phosphorylation site affected, which showed different abilities to bind sRNAs and have differences in suppressor activity. The deletion of the whole site (mutant 2bΔKSPSE) abolished the suppressor activity of the protein and dramatically reduced its ability to bind RNAs (the apparent K_d for sRNA binding is about four times higher than that of the native 2b protein). In comparison, point substitutions of two serines (Ser40 and Ser42) had no effect on local silencing suppression in vivo and resulted in either a slight increase of RNA binding (mutant 2bS40A) or a moderate reduction (mutant 2bS42A), with apparent K_d 1.2–2 times lower for the latter than in the case of the native 2b protein. According to the structural model of the 2b protein, the site of interaction with ds siRNA is formed by two α-helices and a linker between them in the N-terminal half of the 2b protein (Chen et al. 2008). The putative phosphorylation site comprises a part of the linker and part of the second α-helix. Deletion of the whole KSPSE motif had a dramatic effect preventing the normal formation of the functionally active complex between the ds siRNA and the protein, which likely is the cause of its inability to function as a suppressor. This is probably due largely to the invariant P41 of the KSPSE motif, since Chen et al. (2008) also showed that substitution of P41 by alanine greatly reduced silencing suppression of the TAV 2bP41A mutant protein and also reduced the binding affinity for siRNA 10-fold. The P41 generates a kink in the protein backbone following the first α-helix, which allows the second α-helix to also bind to part of the ds siRNA (Chen et al. 2008). Interestingly, in contrast to the effect on the binding of sRNAs, the 2bΔKSPSE mutation had an even more pronounced effect (complete abolishment) on the interaction with a long viral RNA (Fig. 4).

Binding to TMV RNA produced only two kinetic patterns: One pattern was exhibited by the four mutants that retained suppression of silencing activity (2bS40A, 2bS42A, 2bΔGSEL, and 2bΔ3T) plus the native protein, and the other pattern was shown by the four mutants that lacked silencing suppressor activity (2bΔNLS1, 2bΔNLS2, 2bΔNLS1 + 2, 2bΔKSPSE), which showed very weak binding only. In the former case, binding was noneffective, although cooperative, and suggested a binding by the various proteins much weaker than was observed against sRNAs (Fig. 4). At the moment, we do not know how the interaction of the 2b protein with TMV RNA relates to the binding of some viral movement proteins to genomic viral RNAs.

Tagging of GFP–2b with an NES resulted in the relocation of the protein from the nucleus/nucleolus into the cytoplasm (Fig. 5). The patch assays showed that NES–GFP–2b retained its ability to suppress RNA silencing (Fig. 6). In fact, at the time points studied the steady-state levels of free GFP reporter were comparable in the presence of NES–GFP–2b as in that of GFP–2b (Fig. 6). Therefore, we have shown that the cytoplasmic 2b protein construct retained the same suppressor activity in the patch assays as a construct that has nuclear/nucleolar accumulation. These results also showed that the effect of the NES is stronger than that of the two NLSs, and that it shifts the transit to the nucleus toward the cytoplasm. For this reason we cannot exclude that nuclear import (or transit through the nucleus) is still required for the 2b protein to acquire suppression of silencing activity, since the NLSs were retained in the NES-tagged construct. However, we demonstrated that sustained presence of the 2b protein in the nucleus is not required for the local suppression of silencing activity of the 2b protein of Fny CMV. On the other hand, our RNA binding kinetic studies suggest that the 2b protein suppression activity is related to its ability to bind to sRNAs, which presumably would take place in the cytoplasm. Interestingly, binding and inhibition of AGO1

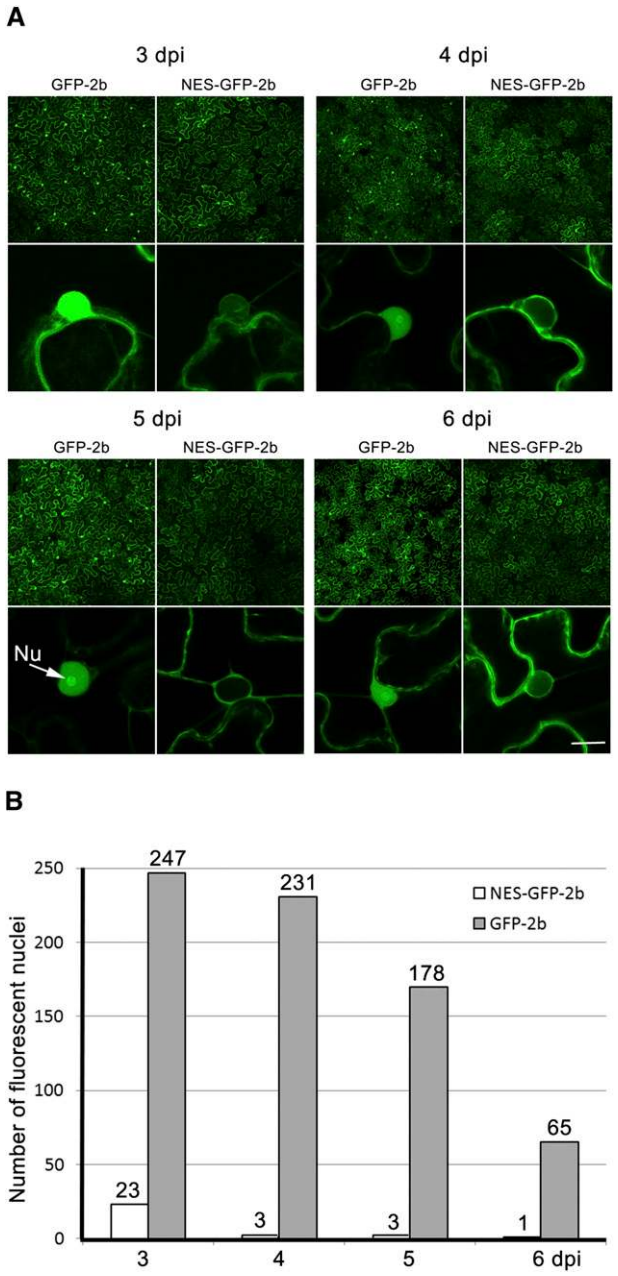

FIGURE 5. (*A*) Alterations in the subcellular localization patterns of a 2b protein tagged with *Aquorea victoria green fluorescent protein* (GFP–2b) with or without a NES at its N terminus (constructs NES–GFP–2b vs. GFP–2b, respectively). Both constructs were transiently expressed from agroinfiltrated binary vectors in *N. benthamiana*. Observations were made with a confocal microscope at 3, 4, 5, and 6 dpi. Fields of epidermal cells 750 × 750 μm in size are shown in the *upper* panel rows. All field images (but not those of nuclear close-up views) were taken under the same confocal settings, and can be directly compared. The *lower* panel row shows close-up views of representative individual nuclei. The nucleolus (Nu) is indicated by an arrow. Note that in the case of NES–GFP–2b fluorescence is absent from inside the nuclei, including nucleoli. Bar in the *lower right* corner represents 10 μm. (*B*) At 3, 4, 5, and 6 dpi, and for both constructs NES–GFP–2b and GFP–2b, four separate randomly chosen fields of epidermal cells (750 × 750 μm) were screened for nuclei that showed fluorescence inside them. Each field contains ~50–80 cells, depending on leaf age. Results are displayed in the chart as the total number of fluorescent nuclei detected.

have been shown to be another level at which the 2b protein could interfere with silencing (Zhang et al. 2006); AGO1 is a cytoplasmic protein and the interaction with 2b protein has been visualized there (González et al. 2010).

What then would be the role of the nuclear targeting of the 2b protein? As we mentioned in the Introduction, this small molecule causes various effects with a complex interactome, and the nuclear targeting of the protein could have roles in the viral infectious cycle that may or may not be related to the suppression of silencing function of the protein. In this regard, it may be relevant that the 2b protein can interact with a cytoplasmic catalase and translocate it into the nucleus (Inaba et al. 2011), much in the way the tombusviral P19 can alter the subcellular localization of ALY proteins (Canto et al. 2006). This translocation also seems unrelated to silencing suppression. However, it also has been demonstrated that the 2b protein can translocate sRNAs from the cytoplasm into the nucleus (Kanazawa et al. 2011) and this property has been used to engineer the inheritable methylation of endogenous gene promoters (Kanazawa et al. 2011). It could therefore be possible that transport of siRNAs and miRNAs to the nucleus could be aimed either at their functional removal from the cytoplasm, or with the intent of causing specific effect in the nucleus, such as perhaps interference with DNA methylation (Guo and Ding 2002). In addition, interaction of 2b with AGO4 has been demonstrated in vivo and visualized inside the nucleus (González et al. 2010; Hamera et al. 2012) and this interaction could also constitute another link between nuclear localization and suppression of silencing-mediated interference with gene expression, as reported (Cillo et al. 2009; Ye et al. 2009).

MATERIALS AND METHODS

Plasmid constructs

For transient expression in plants, proteins were cloned into the 35S promoter-polylinker-Nos terminator T-DNA cassette of pROK2-based binary vectors. Cloning of the native 2b protein from Fny CMV and of six 2b mutant variants (2bΔNLS1, 2bΔNLS2, 2bΔNLS1 + 2, 2bΔKSPSE, 2bS40A, and 2bS42A) has already been described (González et al. 2010). For the generation of 2b mutant ΔGSEL, the gene sequences flanking the 2b protein GSEL deletion site were amplified by PCR using appropriate oligos, cleaned, kinased and ligated with T4 DNA ligase. The ligation reaction was then used as template for a PCR using only the two oligos at the 5′ end of the upstream PCR product and at the 3′ end of the downstream PCR product. The fusion PCR fragment thus obtained was digested with the appropriate enzymes and cloned in pROK2, and pROK2 harboring *GFP* (pROK–GFP) to generate pROK2 constructs 2b–ΔGSEL and GFP–2bΔGSEL, respectively. To substitute 2bΔGSEL for the native 2b protein in the full-length infectious clone of Fny CMV RNA 2 (pF209) a similar approach was used, only the two PCR products flanking the GSEL deletion site in the *2b* gene extended from nucleotide 1621 of the CMV RNA 2 sequence (upstream fragment) to the 3′ end of the viral sequence

(downstream fragment). Both fragments were cleaned, kinased, and ligated, and the ligation product served as template for the amplification of the fusion PCR product using only the two oligos at the 5′ end of the upstream PCR fragment and at the 3′ end of the downstream PCR fragment. The fusion PCR product thus obtained was digested with NcoI and PstI and cloned into linearized pF209. For the cloning of 2b protein mutant 2bΔ3T into pROK2 and pROK2 harboring GFP (pROK–GFP) the gene was amplified by PCR from a plasmid harboring full-length cDNA for mutant CMV RNA 2 Δ3T (Lewsey et al. 2009) with appropriate flanking restriction enzymes, and ligated into the corresponding linearized plasmids to generate pROK2 constructs 2bΔ3T and GFP–2bΔ3T.

To create 2b proteins tagged with a NES, the NES from the protein kinase inhibitor PKI (Asn–Glu–Leu–Ala–Leu–Lys–Leu–Ala–Gly–Leu–Asp–Ile–Asn–Lys–Thr–Ala; Wen et al. 1995) was amplified by PCR using two partially overlapping oligos, which added an ATG (methionine codon) and an upstream NheI site at its 5′ end and an XbaI site at its 3′ end, respectively. The PCR fragment was digested with these two enzymes and cloned into XbaI-linearized, pROK2-based constructs GFP–2b (González et al. 2010), generating pROK2 constructs NES–GFP–2b and NES–GFP–2bΔKSPSE, respectively. Both contain the NES signal at their N termini. In addition, the ATG at the start of the *GFP–2b* was removed to prevent the occurrence of ribosomal internal initiation events.

All GFP-tagged constructs harbored a GFP variant (Tu65, Clontech), which did not allow them to be detected under the UV lamp. For UV lamp detection of fluorescence from a free GFP reporter gene in the agroinfiltration patch assays, a binary vector expressing eGFP was used (González et al. 2010).

Cloning of native 2b and of the six 2b protein mutants (2bΔNLS1, 2bΔNLS2, 2bΔNLS1 + 2, 2bΔKSPSE, 2bS40A, and 2bS42A) in the pQE30 expression vector for protein expression in *E. coli* and purification using a 6xHis tag at their N termini has already been described (González et al. 2010). Cloning of two new 2b protein mutants (2bΔGSEL and 2bΔ3T) was achieved in a similar way, with both genes transferred from the pROK2-based constructs into BamHI–SacI-linearized pQE30 expression plasmids (Qiagen).

Transient expression of genes in plant tissues

Cultures of *Agrobacterium tumefaciens* C58C1 containing binary vectors were grown to exponential phase in LB medium with antibiotics at 28°C. For infiltration, each bacterial culture harboring a different T-DNA was diluted to a final OD of 0.2 at 600 nm. Different cultures harboring different T-DNAs were then combined and infiltration of the mixtures was performed on fully expanded leaves of *N. benthamiana* plants using a syringe as described (Canto et al. 2002).

Imaging of fluorescence from tagged proteins in cells and tissues

Epidermal cells in *N. benthamiana* infiltrated tissue were monitored for fluorescence derived from GFP, or mRFP-tagged proteins at 3–6 dpi. Imaging was conducted with Leica SP2 and SP5 (Leica Microsystems) confocal laser scanning microscopes and software, using fresh, nontreated leaf tissue, and 20× magnification water immersion or 40× water dipping objectives, as described previously (González et al. 2010).

Local suppression of silencing in agroinfiltrated patch assays

A free *GFP* reporter gene expressed from a binary vector under the control of the 35S promoter was expressed transiently in a *N. benthamiana* leaf, either co-infiltrated with the empty binary vector pROK2 (right side of leaf), or with another vector expressing a protein to be tested for suppression of silencing

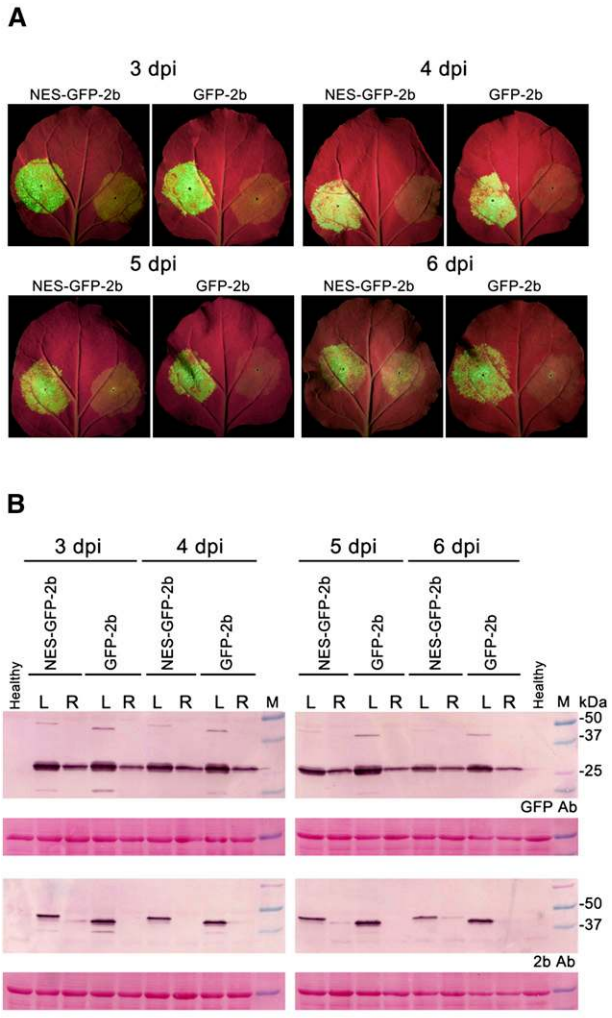

C

Increase in free GFP band density	Suppressor	Observed	Expected*
3 dpi	GFP-2b	X 2.24	
	NES-GFP-2b	X 1.73	X 1.43
4 dpi	GFP-2b	X 1.9	
	NES-GFP-2b	X 1.44	X 1.58
5 dpi	GFP-2b	X 2.5	
	NES-GFP-2b	X 1.40	X 1.65
6 dpi	GFP-2b	X 2.5	
	NES-GFP-2b	X 1.43	X 1.35

*From the ratio of NES-GFP-2b to GFP-2b band densities

FIGURE 6. (Legend on next page)

activity (left side of leaf). To monitor the effect of the second protein on the levels of fluorescence derived from the transiently expressed free eGFP, leaves were illuminated at 3–6 dpi with a Blak Ray long wave UV lamp (UVP) and photographed as previously described (Canto et al. 2002; González et al. 2010).

Immunoblot detection of proteins and analysis

Total protein content from infiltrated tissue was extracted with a pestle in Laemmli buffer, and the sample was boiled and fractionated in SDS-PAGE 15% gels. Gel proteins were wet-blotted in Tris-glycine buffer onto Hybond-P PVDF membranes (Cat. RPN303F, Amersham, GE Healthcare). For immunological detection of GFP, a rabbit GFP polyclonal antiserum kindly donated by G. Cowan (James Hutton Institute, Dundee, UK) was used. For detection of the Fny CMV 2b protein, a mouse polyclonal antiserum raised against both the N and C domains of the protein (amino acids 2–58 and 51–107, respectively) was used (González et al. 2010). Blotted proteins were detected using commercial alkaline phosphatase-conjugated secondary antibodies and SigmaFast BICP/NBT substrate tablets (Cat. B5655, SIGMA Aldrich). Comparative Protein densitometric analysis of blotted proteins was made with the Quantity One 4.6.3 1-D analysis software (Bio-Rad laboratories).

Bacterial protein expression and gel-shift RNA-binding assays

Native and mutant 2b proteins were expressed from plasmid pQE30 in *E. coli* and purified using the 6×His tags at their N termini and Ni-NTA chromatography (Qiagen) followed by renaturation by dialysis, as described (Rakitina et al. 2006; González et al. 2010). For gel-shift sRNA binding assays, three 21-nt small RNAs based on the sequence of miRNA 171 were synthesized: UGAUUGAGCCGCGCCAAUAUC, UAUUGGCGC GGCUCAAUCAGA, UAUUGGCCUGGUUCACUCAGA. Synthetic ds siRNAs and miRNAs were formed by mixing equimolar amounts of the corresponding small RNAs, followed by boiling and cooling slowly to room temperature. For in vitro Protein–siRNA binding assays, 5 pmol of synthetic ds sRNAs (15 pmol of ss sRNA) or 0.5 μg of TMV viral RNA were used. RNA and protein were mixed at various ratios in RNA binding buffer (20 mM Tris-HCl pH 7.5; 1 mM dithiothreitol; 3 mM $MgCl_2$; 50 mM NaCl), incubated for 15 min on ice and were then analyzed in either 2% or 0.8% agarose Tris-acetate gels for sRNAs or TMV RNA, respectively, as described (Rakitina et al. 2006). RNAs in gels were detected by

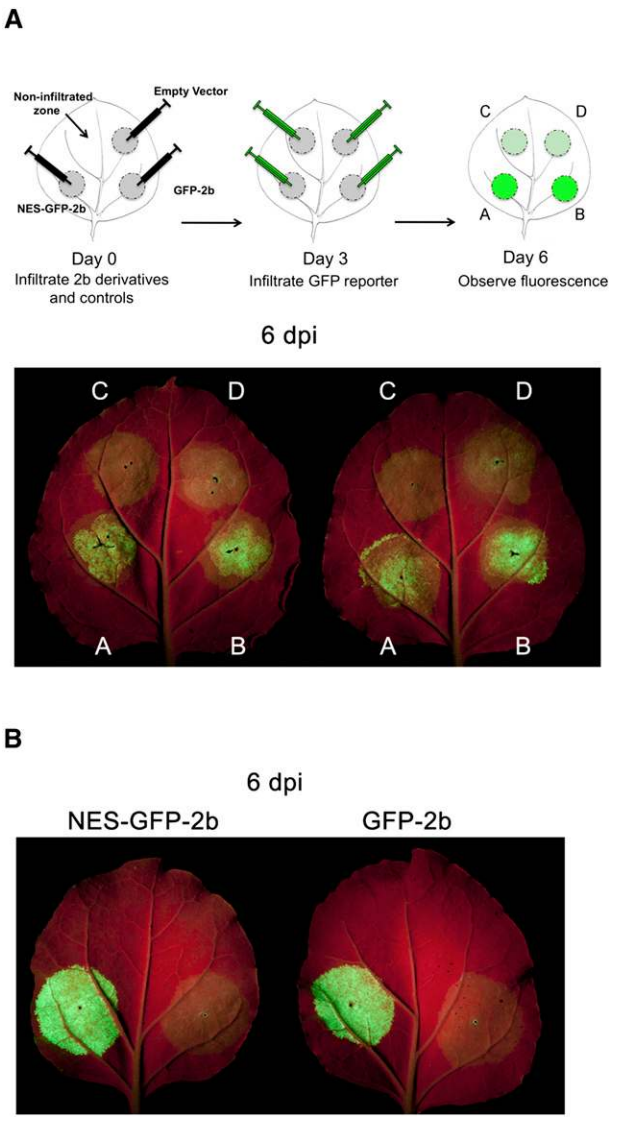

FIGURE 6. Comparative suppression of local RNA silencing by GFP–2b and NES–GFP–2b in patch assays. A binary vector expressing the *GFP* reporter gene was agroinfiltrated in *N. benthamiana* leaves, together with an empty binary vector (infiltrated patch in *right* side of leaves) or together with binary vectors expressing either NES–GFP–2b or GFP–2b (infiltrated patch in *left* side of leaves). (*A*) Leaves photographed under UV light at 3, 4, 5, or 6 dpi. (*B*) Western blot analysis of the accumulation of the GFP reporter and of the 2b fusion proteins NES–GFP–2b and GFP–2b at 3, 4, 5, and 6 dpi. Total protein samples were analyzed with antibodies against GFP (*upper* panels) or the 2b protein (*lower* panels). Lanes labeled *L* and *R* correspond to the infiltrated patches in *left* and *right* side of leaves, respectively. Lanes *H* and *M* stand for healthy plant extract and molecular weight markers, respectively. The panels *below* each blot show the Ponceau S stained membranes as control of loading. (*C*) Summary of the conclusions from the densitometric analysis of the Western blot protein bands corresponding to free GFP, NES–GFP–2b, and GFP–2b. This shows the increases in free GFP accumulation induced by GFP–2b at 3, 4, 5, and 6 dpi. It also shows the increases expected for NES–GFP–2b if it were to suppress silencing as GFP–2b did, based on each suppressor relative accumulation, and the ones actually observed.

FIGURE 7. Comparative suppression of local RNA silencing by GFP–2b and NES–GFP–2b in a sequential patch assay. (*A*) *N. benthamiana* leaves were serially agroinfiltrated in the same area twice. First, leaves were agroinfiltrated with binary vectors expressing either NES–GFP–2b or GFP–2b (patches A and B, respectively); another area of the leaf was left uninfiltrated (patch C) and a fourth area was infiltrated with *Agrobacterium* harboring no binary vector (patch D). Three days after the infiltration (dpi), the four patches A to D were agroinfiltrated again with a binary vector expressing a reporter GFP, and after three further days (day 6) samples were monitored for fluorescence derived from the reporter GFP under the UV lamp. Two identically treated leaves are shown. GFP fluorescence enhanced similarly in patches A and B, when compared to patches C and D. (*B*) As a control, the suppression of the silencing of the reporter GFP at 6 dpi, when co-infiltrated at time 0 with either an empty binary vector (*right* side of both leaves) or the binaries expressing NES–GFP–2b or GFP–2b (*left* side of corresponding leaves).

staining them with ethidium bromide. Digital images of the gels were taken and the amount of free nonretarded RNA was quantified with the program Gel-Pro analyzer (version 3.1.00.00, Media Cybernetics) to obtain the retardation curves. Data thus obtained were used to obtain the Hill coefficients to measure cooperativity (<1, non-cooperative binding; >1, cooperative binding), and apparent K_d, understood as protein concentration at which 50% RNA is bound. To determine the apparent K_d values, the data points were fitted using the Hill equation by SigmaPlot 11 (Systat Software Inc. [SSI]), where the fraction bound = $1/(1 + (K_d^n/[\text{Protein concentration}]^n)$, and n represents the Hill constant.

ACKNOWLEDGMENTS

This work was supported by a joint grant between the Spanish National Research Council (CSIC)–Russian Foundation for Basic Research (2008RU0089; 09-04-91285-INIS_a) and grants from the Spanish Ministry of Innovation and Science (AGL2008-03482; ACI2009-0855). The work of M.T. is funded by the Scottish Government's Rural and Environment Science and Analytical Services (RESAS) Division. I.G. was a recipient of a JAEpre PhD fellowship from CSIC. We thank an anonymous referee of González et al. (2010) for the suggestion to tag the 2b protein with a NES.

Received November 8, 2011; accepted December 28, 2011.

REFERENCES

Brigneti G, Voinnet O, Li WX, Ding SW, Baulcombe DC. 1998. Viral pathogenicity determinants are suppressors of transgene silencing in *Nicotiana benthamiana*. *EMBO J* **17:** 6739–6746.

Canto T, Cillo F, Palukaitis P. 2002. Generation of siRNAs by T-DNA sequences does not require active transcription or homology to sequences in the plant. *Mol Plant Microbe Interact* **15:** 1137–1145.

Canto T, Uhrig J, Swanson M, Wright KM, MacFarlane SA. 2006. Translocation of *Tomato bushy stunt virus* P19 protein into the nucleus by ALY proteins compromises its silencing suppressor activity. *J Virol* **80:** 9064–9072.

Chen H-Y, Yang J, Lin C, Yuan A. 2008. Structural basis for RNA-silencing suppression by *Tomato aspermy virus* protein 2b. *EMBO Rep* **9:** 754–760.

Cillo F, Mascia T, Pasciuto MM, Gallitelli D. 2009. Differential effects of mild and severe *Cucumber mosaic virus* strains in the perturbation of micro RNA-regulated gene expression in tomato map to the 3′ sequence of RNA 2. *Mol Plant Microbe Interact* **22:** 1239–1249.

Díaz-Pendón JA, Li F, Li W-X, Ding S-W. 2007. Suppression of antiviral silencing by *Cucumber mosaic virus* 2b protein in *Arabidopsis* is associated with drastically reduced accumulation of three classes of viral small interfering RNAs. *Plant Cell* **19:** 2053–2064.

García AV, Blanvillain-Baufumé S, Huibers RP, Wiemer M, Li G, Gobbato E, Rietz S, Parker EP. 2009. Balanced nuclear and cytoplasmic activities of EDS1 are required for a complete plant innate immune response. *PLoS Pathog* **6:** e1000970. doi: 10.1371/journal.ppat.1000970.

González I, Martínez L, Rakitina DV, Lewsey MG, Atienzo FA, Llave C, Kalinina NO, Carr JP, Palukaitis P, Canto T. 2010. *Cucumber mosaic virus* 2b protein subcellular targets and interactions: Their significance to RNA silencing suppressor activity. *Mol Plant Microbe Interact* **23:** 294–303.

Goto K, Kobori T, Kosaka Y, Natsuaki T, Masuta C. 2007. Characterisation of silencing suppressor 2b of *Cucumber mosaic virus* based on examination of its small RNA-binding abilities. *Plant Cell Physiol* **48:** 1050–1060.

Guo HS, Ding SW. 2002. A viral protein inhibits the long range signalling activity of the gene silencing signal. *EMBO J* **21:** 398–407.

Ham BK, Lee TH, You JS, Nam YW, Kim JK, Paek KH. 1999. Isolation of a putative tobacco host factor interacting with cucumber mosaic virus-encoded 2b protein by yeast two-hybrid screening. *Mol Cells* **9:** 548–555.

Hamera S, Song X, Su L, Chen X, Fang R. 2012. Cucumber mosaic virus suppressor 2b binds to AGO4-related small RNAs and impairs AGO4 activities. *Plant J* **69:** 104–115.

Inaba J, Kim BM, Shimura H, Masuta C. 2011. Virus-induced necrosis is a consequence of direct protein–protein interaction between a viral RNA-silencing suppressor and a host catalase. *Plant Physiol* **156:** 2026–2036.

Ji LH, Ding SW. 2001. The suppressor of transgene RNA silencing encoded by *Cucumber mosaic virus* interferes with salicylic acid-mediated virus resistance. *Mol Plant Microbe Interact* **14:** 715–724.

Kanazawa A, Inaba J, Shimura H, Otagaki S, Tsukahara S, Matsuzawa A, Kim BM, Goto K, Masuta C. 2011. Virus-mediated efficient induction of epigenetic modifications of endogenous genes with phenotypic changes in plants. *Plant J* **65:** 156–168.

Lewsey M, Robertson FC, Canto T, Palukaitis P, Carr JP. 2007. Selective targeting of miRNA-regulated plant development by a viral counter-silencing protein. *Plant J* **50:** 240–252.

Lewsey M, Surette M, Robertson FC, Ziebell H, Choi SH, Ryu KH, Canto T, Palukaitis P, Payne T, Walsh JA, et al. 2009. The role of the *Cucumber mosaic virus* 2b protein in viral movement and symptom induction. *Mol Plant Microbe Interact* **22:** 642–654.

Lewsey MG, Murphy AM, MacLean D, Dalchau N, Westwood JH, Macaulay K, Bennet MH, Moulin M, Hanke DE, Powell G, et al. 2010. Disruption of two defensive signaling pathways by a viral RNA silencing suppressor. *Mol Plant Microbe Interact* **23:** 835–845.

Lucy AP, Guo H-S, Li W-X, Ding S-W. 2000. Suppression of post-transcriptional gene silencing by a plant viral protein localized in the nucleus. *EMBO J* **19:** 1672–1680.

Mayers CN, Palukaitis P, Carr JP. 2000. Subcellular distribution analysis of the cucumber mosaic virus 2b protein. *J Gen Virol* **81:** 219–226.

Rakitina DV, Yelibna NE, Kalinina NO. 2006. Zinc ions stimulate the cooperative RNA binding of hordeiviral γb protein. *FEBS Lett* **580:** 5077–5083.

Rashid UJ, Hoffman J, Brutschy B, Piehler J, Chen JC-H. 2008. Multiple targets for suppression of RNA interference by *Tomato aspermy virus* protein 2b. *Biochemistry* **48:** 12655–12657.

Shi B-J, Symons RH, Palukaitis P. 2008. The cucumovirus 2b gene drives selection of inter-viral recombinants affecting the crossover site, the acceptor RNA and the rate of selection. *Nucleic Acids Res* **36:** 1057–1071.

Shimura H, Fukagawa T, Meguro A, Yamada H, Oh-hira M, Sano S, Masuta C. 2008. A strategy for screening an inhibitor of viral silencing suppressors, which attenuates symptom development of plant viruses. *FEBS Lett* **582:** 4047–4052.

Sueda K, Shimura H, Megura A, Uchida T, Inaba J-I, Masuta C. 2010. The C-terminal residues of the 2b protein of *Cucumber mosaic virus* are important for efficient expression in *Escherichia coli* and DNA binding. *FEBS Lett* **584:** 945–950.

Wang Y, Tzfira T, Gaba V, Citovsky V, Palukaitis P, Gal-On A. 2004. Functional analysis of the *Cucumber mosaic virus* 2b protein: Pathogenicity and nuclear localization. *J Gen Virol* **85:** 3135–3147.

Wen W, Meinkoth JL, Tsien RY, Taylor S. 1995. Identification of a signal for rapid export of proteins from the nucleus. *Cell* **82:** 463–473.

Ye J, Qua J, Zhang J-F, Geng Y-F, Fang R-X. 2009. A critical domain of the *Cucumber mosaic virus* 2b protein for RNA silencing suppressor activity. *FEBS Lett* **583:** 101–106.

Zhang X, Yuan Y-R, Pei Y, Lin S-S, Tuschl T, Patel DJ, Chua N-H. 2006. *Cucumber mosaic virus*-encoded 2b suppressor inhibits *Arabidopsis* Argonaute1 cleavage activity to counter plant defense. *Genes Dev* **20:** 3255–3268.